

図1 ヒトiPS細胞から成熟心筋細胞の分化誘導法  
ヒトiPS細胞からサイトカインなどの液性因子や遺伝子導入などの方法を用いて、段階的に心筋細胞に分化誘導できる。

る<sup>5)</sup>。我々は成体心室筋と比較してiPS由来分化心筋細胞において不足している因子Xに着目し、心筋細胞の成熟化を誘導できる方法を明らかにしている(論文投稿中)。我々が検討した範囲では、アデノウイルスは未分化iPS細胞よりも分化が進んだ細胞の方が高い感染効率を示したことから、iPS由来分化心筋細胞にアデノウイルスを用いて因子Xを遺伝子導入することにより、成熟心筋を誘導することに成功した。ただし、医薬品の催不整脈作用を評価する上で成熟心筋の方がいいのかはまだ分かっていない。一般的にはヒト成体の心筋細胞に近ければ近い方が創薬のモデルとして良さそうであるが、本当に成熟した特性が必要なのかは以下に述べるような薬理作用の観点から判断すべきであろう。

#### 4. 分化心筋細胞を用いた*in vitro*心毒性試験

*In vitro*心毒性試験に用いるiPS由来分化心筋細胞の形状としては、個々の細胞、EBなどの細胞塊、高密度培養によるシート状の標本などがあげられる。個々の細胞の場合は、パッチクランプで一つ一つの細胞の活動電位の波形をもとにQT間隔を評価するため、心室筋などのサブタイプの情報も得られる。しかしながら、スループット性は極めて低いこと、個々の細胞のバラつきの問題があること、長時間曝露による薬理作用も検討できないことなど多くの問題があり、現実的ではないように思われる。

一方、細胞塊やシート状の標本に関しては、多点電極システムを用いて、電極を埋め込んだディッシュに細胞塊やシートを接着させることによりQT間隔に相当する細胞外電位(Field Potential: FP)の測定が可能である。個々の心筋細胞のバラつきが平均化されるため、比較的安定したデータが得られること、侵襲がないため長時間曝露による薬理作用が調べられること、電気生理学特有の敷居の高さは

なく比較的簡便であることなど、先程の問題点はかなり克服できる。我々が検討した範囲では、細胞塊は電極の上うまく乗せられなかったり、細胞塊と電極の接触が不十分でシグナルが得られないようなケースがあったことから、シート状の標本の方がベターではないか、と考えている。ただし、多点電極システムを用いるにしても、一日で解析できる数に限界があり、大規模な医薬品候補化合物のスクリーニングには向いていない。今後、スループット性を上げるために改良が必要である。

我々は、iPS由来分化心筋細胞を用いた試験系の検出感度を明らかにするため、シート状に播種したiCell心筋細胞をモデル細胞として用いて、細胞外電位装置による評価を行った<sup>6)</sup>。産官学の3施設で検証した結果、どの施設においてもhERG阻害剤E-4031の添加により濃度依存的にFPD(Field Potential Duration)延長が観察された(図2)。さらに、E-4031によりEarly afterdepolarization (EAD)やtriggered activityなどの異常な波形を検出できることが明らかになった(図3)。こちらはFPDとは異なり、既存の*in vitro*評価系では検出できないような不整脈のリスク評価につながると考えられ、非常に興味深い。現在、我々は成熟した分化心筋細胞を用いて同様のアッセイを行っており、催不整脈作用の評価に成熟心筋の特性が必要なのか明らかにする予定である。

今後、多点電極システムを用いた試験法の確立に向けて大規模なバリデーションを実施する場合、様々な実験条件を揃える必要がある。例えば、自律拍動なのかペーシングなのか、細胞の播種密度や培養期間、FPDの解析パラメーターの選択、EADの波形基準などがあげられる。特に、EADにおいては統一的な波形の判定基準の見解が得られていないので、波形の目合わせを行って情報を共有しながら

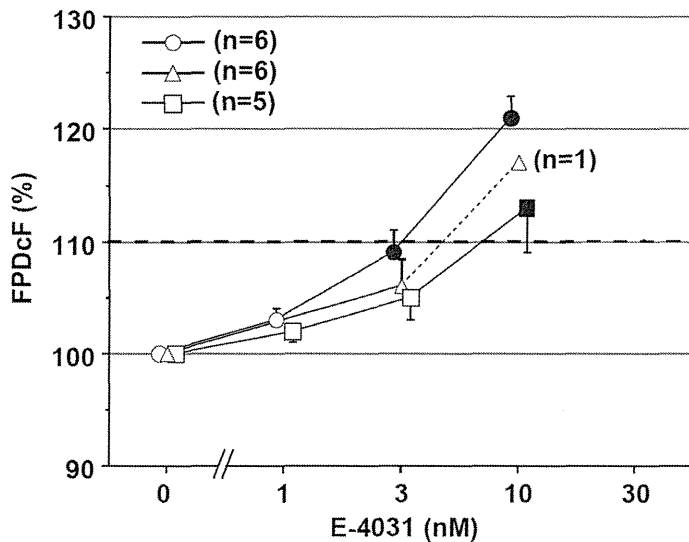


図2 E-4031によるFPD延長  
各施設において、hERG阻害剤E-4031によってFPDの延長が認められた。

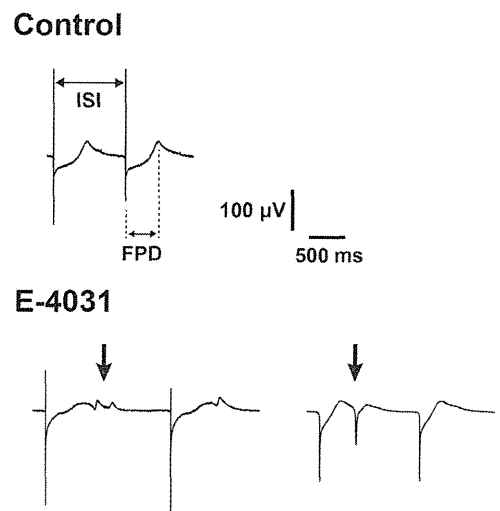


図3 E-4031による異常波形  
E-4031によって、Triggered activityやEarly afterdepolarizationなどの異常な波形が認められた。

設定する必要があると思われる。

なお、今回は多点電極のデータを紹介したが、それ以外にも膜電位感受性色素やカルシウムイメージング、心収縮など様々な薬理評価法があり、陽性対照物質、陰性対照物質などのデータをもとに再現性や信頼性を評価していく必要がある。2013年に発足した製薬協タスクフォース(TF-5)においても様々な検証が行われており、今後の解析を待ちたい。

## 5. ガイドラインに向けた展望

ここ数年、ヒトiPS細胞を使った心毒性試験に関する発表が相次ぎ、iPS由来分化心筋細胞が催不整脈作用の評価に使えるのではないかと、いう機運が高まってきている。さらに、2013年7月から、FDA/HESI/CSRC\*においてCiPA (Comprehensive *in vitro* Proarrhythmia Assay) の枠組みが発足し、薬剤による不整脈誘発リスク評価に関して国際的な議論も開始された<sup>7,8)</sup>。特に、S7Bガイドラインの改定やE14ガイドラインの廃止などを見据えることを明言している。現在市販されている分化心筋細胞はメーカーの差やロット差等があるとされるが、良い細胞がないから議論できない、では全く前に進まないのか、発想を変えて、今ある細胞で何ができるのか? を考える時期に来ている。日本としても、国内におけるiPS由来分化心筋細胞の大量かつ安定

な供給体制を整備するとともに、多くの薬剤に対する心毒性データを揃えて、国際協調をはかりながらiPS細胞の実用化をすすめていく必要がある。

## 6. まとめ

ヒトiPS細胞の分化誘導技術などの研究が進展し、またCiPAなどの国際的な議論も開始されたことにより、ヒトiPS細胞を心毒性試験に利用する機運が高まってきている。日本としても、ガイドライン化を見据えて科学的な根拠をしっかりと確保しておかなければならない。将来的には、日本発のヒトiPS細胞技術を用いて、心毒性の発生を回避することが可能となり、より安全な医薬品が提供されることを期待したい。

## 7. 謝辞

本研究は、国立医薬品食品衛生研究所薬理部 関野祐子先生、東京医科歯科大学難治疾患研究所生体情報薬理分野 古川哲史先生 黒川洵子先生、東邦大学医学部薬理学講座 杉山篤先生 安東賢太郎先生 中村裕二先生、エーザイ株式会社 澤田光平先生 宮本憲優先生、株式会社新日本科学 松尾純子先生との共同研究です。深く感謝申し上げます。また、2014年1月に開催された第1回心臓安全性に関するシンクタンクミーティング2014 in 霧島に参加

\* FDA: Food and Drug Administration  
HESI: Health and Environmental sciences Institute  
CSRC: Cardiac Safety Research Consortium

された方々との討論も大変参考になりました。この場をお借りして感謝申し上げます。

#### 参考文献

- 1) Bock C, Kiskinis E, et al : Reference Maps of human ES and iPS cell variation enable high-throughput characterization of pluripotent cell lines. *Cell* 2011.144.439-452.
- 2) Ferri N, Siegl P, et al : Drug attrition during pre-clinical and clinical development: understanding and managing drug-induced cardiotoxicity. *Pharmacol Ther* 2013.138.470-84.
- 3) Burridge PW, Keller G, et al : Production of de novo cardiomyocytes: human pluripotent stem cell differentiation and direct reprogramming. *Cell Stem Cell* 2012.10:16-28.
- 4) Uosaki H, Fukushima H, et al : Efficient and scalable purification of cardiomyocytes from human embryonic and induced pluripotent stem cells by VCAM1 surface expression. *PLoS ONE* 2011;6:e23657.
- 5) Lieu DK, Fu JD, et al: Mechanism-based facilitated maturation of human pluripotent stem cell-derived cardiomyocytes. *Circ Arrhythm Electrophysiol* 2013.6.191-201.
- 6) Nakamura Y, Matsuo J, et al : Assessment of testing methods for drug-induced repolarization delay and arrhythmias in an iPS cell-derived cardiomyocyte sheet: multi-site validation study. *J Pharmacol Sci* 2014.124.494-501.
- 7) Chi KR. Revolution dawning in cardiotoxicity testing. *Nat Rev Drug Discov* 2013.12.565-567.
- 8) Sager PT, Gintant G, et al : Rechanneling the cardiac proarrhythmia safety paradigm:a meeting report from the Cardiac Safety Research Consortium. *Am Heart J* 2014.167.292-300.

# 再生医療における臨床研究と製品開発

諫田 泰成

国立医薬品食品衛生研究所 薬理部第二室 室長

(株)技術情報協会

「再生心筋細胞を用いた安全性薬理評価系の開発」 抜刷

2013年9月発刊

### 第3節 再生心筋細胞を用いた安全性薬理評価系の開発

はじめに

ヒト iPS 細胞は、今まで入手が困難であったヒト細胞の作製が可能となるため、「再生医療」と「創薬」の実用化が期待されている（図1）。再生医療への注目度は非常に高く、ヒト iPS 細胞から作成した網膜色素上皮細胞を移植する臨床研究が2012年度に申請され、正式に承認された。創薬応用としては、医薬品の安全性や有効性の評価に対する利用が考えられ、創薬プロセスの早い段階で医薬品候補化合物の副作用などを予測できれば、臨床試験における予測性の向上や安全性確保、開発コスト削減などが期待される（図1）。

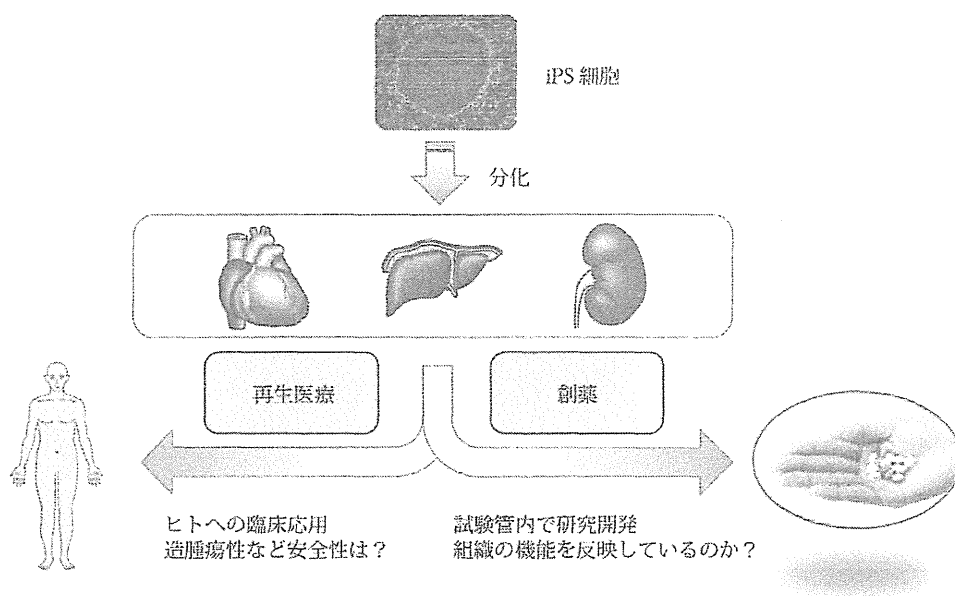


図1 ヒト iPS 細胞の医療応用への可能性

これらのヒト iPS 細胞の実用化に向けた課題として、ヒト未分化 iPS 細胞の品質、すなわち株間の差、継代数や研究室間の差などが明らかになり、国内外のプロジェクトにより標準化の作業が進められている<sup>1)</sup>。しかし、ヒト iPS 細胞由来の分化細胞に関してはほとんど標準化が手付かずであり、分化誘導の標準プロトコールや分化細胞の品質評価、分化指向性などあまり明らかになっていない。

また、再生医療と創薬応用でそれぞれ克服すべき課題も明らかになってきている。再生医療においては、分化細胞の安全性の確保が必須であり、残存している未分化 iPS 細胞の検出など造腫瘍性の評価法の開発が進められている<sup>2)</sup>。分化心筋細胞に関しては、移植によって不整脈が誘発されないかなどの検証も必要である。創薬応用は、in vitro のアッセイ系で分化細胞を使用するため再生医療とは異なり安全面のハードルが低く分化製品に対するウイルス導入などの加工も可能であるが、元の臓器の性質を反映した成熟した細胞が必要と考えられる。

そこで本稿では、ヒト iPS 細胞から心筋細胞への分化誘導技術ならびに分化心筋細胞の電気生理学的特性を概説し、将来的にヒト iPS 細胞の創薬応用実用化に向けて整備すべき課題について考察したい。

#### 1. ヒト iPS 細胞の心筋分化誘導法

##### 1.1 EB 形成法

ヒト iPS 細胞から分化心筋細胞の一般的な作製法として、図2Aに示すような胚様体 (Embryoid body, EB) を形成させる方法が知られている。胚の発生過程を in vitro で模倣するためにマウス ES 細胞から擬似的な胚である EB を形成さ

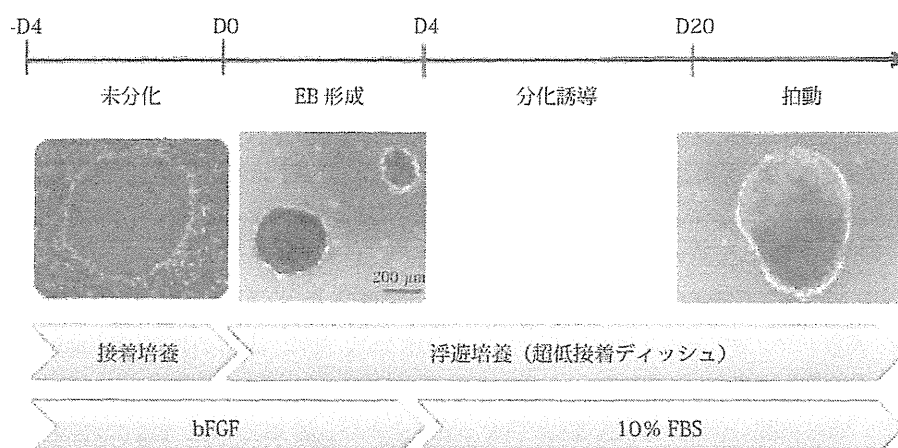
せる方法が開発され、ヒト iPS 細胞にも応用されている。

マウス ES 細胞の場合には、未分化 ES 細胞をトリプシン処理により single cell にして、非接着コート処理済の 96 ウエルプレートなどを用いて EB を形成する。一方、ヒト iPS 細胞の場合には single cell にすると細胞死が起きるため、最初は小さな細胞塊を用いて EB を作成する必要がある。小さな細胞塊はヒト iPS 細胞のコロニーを CTK 溶液（トリプシン、コラーゲナーゼを含む分散液）などで処理した後ピペティングすることによって作製し、低接着ディッシュに移す。すぐに 10% 血清を含む DMEM などの分化培地に変更すると細胞死が誘導されることがあるため、我々は basic fibroblast growth factor (bFGF) を含む未分化維持培地で数日間培養して EB を形成させてから、3 日ごとに半量を分化培地（10% 血清, 0.1mM 2-メルカプトエタノール, 非必須アミノ酸を添加した DMEM）に切り替えている。未分化維持に重要な bFGF の除去により分化スイッチが ON になり、外・中・内胚葉の三方向へ分化が誘導される。中胚葉を経由して心筋にも分化が誘導され、分化培地で EB の培養を続けると 2～3 週間後に拍動する EB が観察される。

EB 法の欠点は、三方向へ分化が誘導されるため、特定の細胞への分化効率が低いことである。EB の中でも心筋細胞は 10% 程度しか含まれていない。そこで、心筋分化効率を高くするために分化を亢進する液性因子が探索され、BMP-4, Wnt3a, G-CSF など様々な因子が報告されている<sup>3-5)</sup>。もう一つの欠点は、EB のサイズが不均一で形状もばらばらであるため、EB 間の差が大きく拍動数などもバラつくことである。我々は EZ passage (Invitrogen #23181-010) を使用してコロニーを処理し、できる限り均一なサイズとなるように心掛けています。最近、V 字型ウエルの中で強制的に EB を形成させるプレートがいくつか報告されており、形やサイズのそろった EB 作成法の開発が期待される。

このように EB 形成を介する分化プロトコールは比較的簡便であり、特別な試薬を用いることなく血清を含む培地で分化誘導も可能であるが、問題点として、ヒト iPS 細胞には分化指向性が存在し、株間で心筋分化能に差が認められることがあげられる。公的な細胞バンクから入手可能な株の中で、201B7 株、253G1 株は心筋分化能が高いが、Tic 株 (JCRB1331) はほとんど拍動が認められないことから、ヒト iPS 細胞には分化の方向性を規定する特性（分化指向性）があると考えられる。Tic 株は肝臓への分化効率が高いと報告されており<sup>6)</sup>、心筋に対しては分化抵抗性を有する可能性がある。分化指向性に関するメカニズムや選別のマーカーなどは明らかになっていないので、今後の研究の進展が待たれる。目的に応じて最適なヒト iPS 細胞株を入手できるように、分化特性も含めた細胞バンクの整備が望まれる。また、そのような情報を共有するシステムも必要である。

A) EB 形成法



B) 定方向分化誘導法



図2 ヒト iPS 細胞の心筋分化誘導法

## 1.2 定方向分化誘導法

定方向分化誘導法とは、液性因子などを用いて特定の方向へ分化を特徴付ける方法であり、心筋細胞の場合は、中胚葉⇒心筋前駆細胞⇒心筋細胞、と段階的に分化誘導を行うことを指す(図2B)。この際、各ステップで添加する液性因子は、心筋細胞の発生過程やES細胞由来分化細胞に発現している受容体などを元にして、液性因子のスクリーニングや最適化が行われている<sup>7)</sup>。

まず、ヒトiPS細胞をマトリゲルでコートしたディッシュに高密度で播種して、数回継代を行うことによりフィーダーをできる限り除去した後、Activinにより中胚葉や内胚葉の元となる原条へ分化誘導する。BMP-4の添加により中胚葉へ分化誘導がかかる。次に、Wnt antagonistであるDickkopf-1(Dkk-1)などにより心筋前駆細胞の方向へ分化を行い、最終的には心筋細胞の拍動が観察される。

EB形成法と比較すると、定方向分化誘導法は拍動までの期間が約1週間と顕著に短縮できる特徴がある。実際、酵素処理により分散しトロポニンで染色すると40%以上の細胞が心筋細胞であることから、分化効率も非常に高いことを確認している。また、接着したまま分化誘導を行うのでシートのような状態となり、ダイナミックな拍動が観察できる。欠点は、分化誘導のステップが増えてEB形成法よりも手間とコストがかかること、ヒトiPS細胞のコロニーの密度により分化効率が大きく異なることなどがあげられる。また、添加する因子は濃度に加えてタイミングも重要である。Wntシグナルは心筋分化の初期には促進的に作用し、後期では抑制的に作用することが知られており、タイミングが合わない場合には全く逆の作用をもたらすことが起こり得る。従って、液性因子を添加する時期・濃度・順序などに関して慎重に最適化する必要がある。

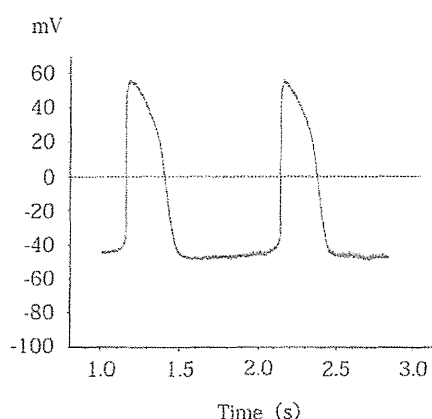
このように心筋細胞への分化プロトコルはEB法、定方向分化法ともに改良が加えられてきているが、分化心筋細胞における遺伝子発現やイオンチャネルの発現は幼若タイプである<sup>8,9)</sup>。後述するように、分化心筋細胞は電気生理学的にも未成熟であるため、現在、我々は成熟させる分化誘導法を構築中である(投稿準備中)。再生医療においては細胞移植により心機能が回復するのが焦点となるので分化細胞の成熟度はあまり問題にならず、むしろ液性因子の産生が重要と言われているが、創薬応用の場合は成熟度が薬剤のスクリーニング効率に影響をあたえる可能性があり、今後の研究に進展が期待される。

## 2. 分化心筋細胞の電気生理学的な特性

一般的に細胞の特性の指標として遺伝子発現やマーカー分子の発現などがあげられるが、心筋細胞で最も重要なことは電気生理学的な特性である。筆者らは創薬応用に向けて、国内の公的な細胞バンクよりヒトiPS細胞株を入手して、分化心筋細胞の品質を検証している。

201B7株由来の拍動EBをピンセットで引っ張るかカッターで刻んだ後にトリプシン処理をするとsingle cellを単離でき、ラミニンでコートしたディッシュに再播種すると拍動する細胞が得られる。この単離拍動細胞を用いてマニュアルパッチクランプにより活動電位を測定したところ、結節、心房、心室型の各サブタイプが存在していることが明らかになった。しかし、心筋細胞の静止膜電位が通常は-90mV程度であるのに対して分化心筋細胞はいずれも-40mV程度と浅いことから、成熟が不十分である可能性が考えられる(図3A)。次に、米国Cellular Dynamics International社で販売されているヒトiPS細胞由来分化心筋細胞(iCell)をiPSアカデミアジャパン株式会社経由で入手し、同様に活動電位の測定を行った。その結果、やはり静止膜電位が浅かったことから(図3B)、元となるiPS細胞の株によるのではなく分化心筋細胞の共通の課題であることが示唆された。

A) 201B7 株由来心筋細胞



B) iCell 心筋細胞

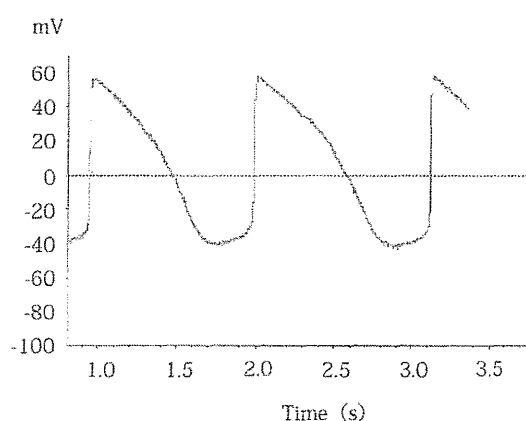


図3 分化心筋細胞の活動電位

このような分化心筋細胞を用いた薬理作用の評価においては、様々なヒト iPS 細胞株から種々の手法を用いて心筋へ分化誘導すると、心筋細胞のサブタイプの割合や成熟度が不均一となり、薬剤に対する反応性についてもばらつくことが予想される。同一の化合物に対して同様の薬理作用が観察できない限り、催不整脈の予測が困難であり、バラつきを抑える必要がある。そこで、我々は次に述べるように、心筋シートを用いた実験プロトコルを整備している。

### 3. 分化心筋細胞を用いた安全性薬理試験

分化心筋細胞を用いた創薬応用の例として、薬剤性不整脈のリスク評価が考えられる。医薬品によって発生する副作用の中でもトルサード・ド・ポアント (TdP) とよばれる重篤な不整脈は重要で、発生頻度は極めて少ないもののまれに心室細動に移行し突然死に至る<sup>10)</sup>。TdP は QT 間隔 (心室の興奮から再分極までの時間) の延長を伴うことから、現在 TdP のリスクは、非臨床試験としてカリウムチャンネル (IKr) を発現させた HEK293 細胞を用いてカリウム電流阻害作用を検討し (hERG 試験法)、次いで *in vivo* で動物の QT 延長作用を評価し、その後臨床において Thorough QT/QTc 試験により厳密にヒトの QT 間隔に対する作用を調べることにより、一定の評価が可能である (図 5)。しかしながら、hERG 試験法は疑陽性が多く、有用な化合物を化合物のスクリーニングのプロセスで除外してしまう可能性がある。ヒト iPS 細胞由来の分化心筋細胞は、カリウム (IKs/IKr) に加えて、カルシウム、ナトリウムなど複数のチャンネルが発現しているため再分極電流への影響を総合的に評価できる利点があり、疑陽性が減少して予測性が向上することが期待される。今までは、心筋への分化誘導条件 (細胞株、分化誘導分化誘導法、日数、培養細胞密度など) が異なるばかりではなく、心筋細胞の電気生理学的機能の測定方法も異なっていたために、実験データを研究間で比較検討ができず、実験結果の再現性を確かめることが困難であった。そこで、我々は電気生理学的特性の解析法を比較検討し、不整脈検出プロトコルの標準化作業を行っている。

個々の心筋細胞の場合は、パッチクランプで解析が可能である。一つ一つの細胞の活動電位の波形をもとに QT 間隔を評価するため、心筋細胞のサブタイプの情報も同時に得られる利点がある。さらに、QT 延長などに起こることが多い早期後脱分極も直接検出することができる。しかし、前述したように個々の波形にバラつきが認められること、スループット性が低く大規模なスクリーニングには向かないこと、侵襲があるので短時間の薬理作用に限定されてしまうことなどを考慮すると、現実的には薬理作用の検出には向かないと考えられる。

細胞塊の場合は、図 4A に示すような多点電極システムを用いて心電図の解析が可能である。電極を埋め込んだディッシュに細胞塊を接着させると、細胞外電位 (Field Potential; FP) が測定できる。FP は細胞内で記録される活動電位の微分波形に一致し、心電図によって得られる信号と同様の変化を記録する事ができる<sup>11)</sup>。従って、ナトリウムによるピークから活動電位再分極時に観察されるカリウムのピークまでの時間である FPD は、心電図における QT 間隔に相当する。



FPDを用いる利点は、侵襲がないため医薬品候補化合物の長時間曝露による薬理作用が調べられることである。しかし、細胞塊ごとのFPの波形が一定の範囲内になるよう均一な塊の作製技術が必要不可欠である。さらに、EBが電極に接していなければシグナルが取得できない。もともと心筋細胞はガラスに張り付きにくい性質がある上に、拍動によってディッシュから剥がれたり接着場所が変わったりするので、ディッシュをコートする基材やデバイスの改善が求められる。我々が作製したヒトiPS細胞由来の拍動EBも市販のヒトES細胞由来細胞塊（スウェーデンCollectis社）も細胞外電位の測定に手間と時間がかかり、スループットも低く、現時点では薬理作用の検出にはまだまだ遠いと言わざるを得ない。

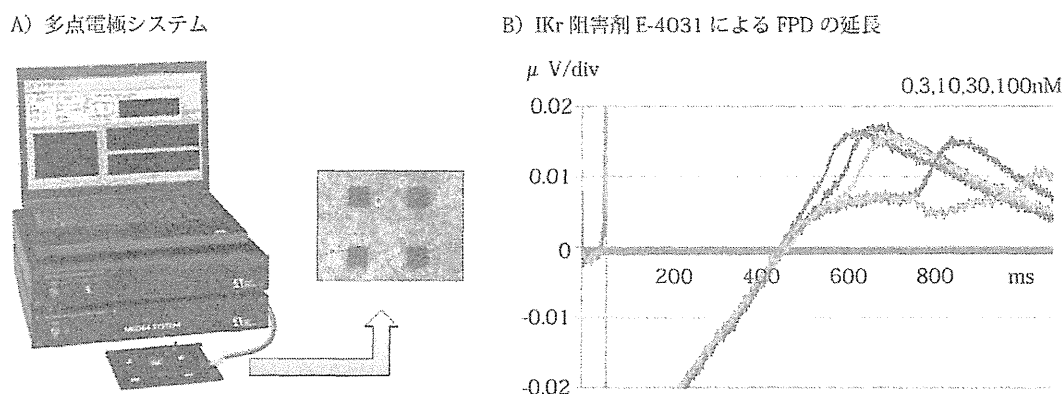


図4 心筋シートにおけるFPの解析

そこで、我々は心筋シートを用いて多点電極システムによるQT延長評価系の開発に着手した。心筋シートは分化心筋細胞を密に播種することで容易に作成することができ同期した拍動が観察される。シート形成によりEB間や個々の心筋細胞などのバラつきが平均化されるため安定したデータが得られると期待される。また、シートは多点電極全体を覆うことになるので、FPのデータ取得も大幅に改善される。実際例として、陽性対照物質であるIKr阻害剤E-4031によって心筋シートのFPD延長が検出できる(図4B)。現在、産官学の枠組みで市販の分化心筋細胞を用いて、薬理作用の再現性、メーカーの相違、ロット間差など比較を行っており、不整脈検出プロトコルの標準化を行っている。

最終的に、分化心筋細胞を用いた試験法として確立するためには、検出感度、再現性、信頼性などを検証する必要がある。検出感度に関しては、今のところ、分化心筋細胞を用いた評価系は感受性が高いような結果が得られており、hERG試験で落とされた医薬品候補化合物を拾えるようなフォローアップに使用できるのかは不明である。再現性や信頼性を明らかにするためには、特定のラボ内のデータのみでは評価できないので、施設内及び多施設間で多くの化合物を用いたバリデーションを行う必要がある。本当に分化心筋細胞を用いる試験系がhERG試験よりも優位性があるのか？分化心筋細胞の試験法が手間やコストをかけるだけの価値があるのか？ヒトにおける予測性が向上するのか？臨床試験を代替しうるのか？などを明らかにしなければならない。

おわりに

ヒトiPS細胞の分化誘導技術などの研究の進展により、ヒトiPS細胞の実用化に向けた動きが盛んである。創薬応用の実用化に向けては、ヒトiPS細胞の株間の差、分化細胞の規格、安全性薬理試験のプロトコル整備など再生医療とは異なる多くの課題が残されている。薬剤性不整脈のリスク評価に関しては、現行のhERG試験法に対する優位性も重要なポイントである。これらの課題を克服することにより、創薬プロセスの効率が向上し、将来的には承認審査の迅速化が実現することが期待される。

## 謝辞

本研究を遂行するにあたり、貴重なご助言とご指導を賜りました国立医薬品食品衛生研究所薬理部 関野祐子部長、東京医科歯科大学難治疾患研究所生体情報薬理分野 古川哲史教授、黒川洵子准教授、エーザイ株式会社 澤田光平博士、宮本憲優博士、株式会社 Ion Chat Research 齋藤光義博士に深く感謝申し上げます。

## 文 献

- 1) Bock C, Kiskinis E, Verstappen G, Gu H, Boulting G, Smith ZD, Ziller M, Croft GF, Amoroso MW, Oakley DH, Gnirke A, Eggan K, Meissner A. *Cell* 144:439-452 (2011)
- 2) Kuroda T, Yasuda S, Kusakawa S, Hirata N, Kanda Y, Suzuki K, Takahashi M, Nishikawa S, Kawamata S, Sato Y. *PLoS ONE* 7:e37342 (2012)
- 3) Takei S, Ichikawa H, Johkura K, Mogi A, No H, Yoshie S, Tomotsune D, Sasaki K. *Am J Physiol.* 296:H1793-H1803 (2009)
- 4) Tran TH, Wang X, Browne C, Zhang Y, Schinke M, Izumo S, Burcin M. *Stem Cells* 27:1869-1878 (2009)
- 5) Shimoji K, Yuasa S, Onizuka T, Hattori F, Tanaka T, Hara M, Ohno Y, Chen H, Egasgira T, Seki T, Yae K, Koshimizu U, Ogawa S, Fukuda K. *Cell Stem Cell* 6:227-237 (2010)
- 6) Inamura M, Kawabata K, Takayama K, Tashiro K, Sakurai F, Katayama K, Toyoda M, Akutsu H, Miyagawa Y, Okita H, Kiyokawa N, Umezawa A, Hayakawa T, Furue MK, Mizuguchi H. *Mol Ther.* 19: 400-407 (2011)
- 7) Fujiwara M, Yan P, Otsuji TG, Narazaki G, Uosaki H, Fukushima H, Kuwahara K, Harada M, Matsuda H, Matsuoka S, Okita K, Takahashi K, Nakagawa M, Ikeda T, Sakata R, Mummery CL, Nakatsuji N, Yamanaka S, Nakao K, Yamashita JK. *PLoS ONE*, 6:e16734 (2011)
- 8) Beqqali A, Kloots J, Ward-van Oostwaard D, Mummery C, Passier R. *Stem Cells*, 24:1956-1967 (2006)
- 9) Cao F, Wagner RA, Wilson KD, Xie X, Fu JD, Drukker M, Lee A, Li RA, Gambhir SS, Weissman IL, Robbins RC, Wu JC. *PLoS ONE*, 3:e3474 (2008)
- 10) Yap YG and Camm AJ. *Heart* 89:1363-1372 (2003)
- 11) Kamp TJ and January CT. *Drug Discovery Today: Disease Mechanisms* 1:45 (2004)

Original Article

## Comparative metabolome analysis of cultured fetal and adult hepatocytes in humans

Su-Ryang Kim<sup>1</sup>, Takashi Kubo<sup>1,4</sup>, Yukie Kuroda<sup>1</sup>, Maki Hojyo<sup>1</sup>, Takuya Matsuo<sup>2</sup>,  
Atsuko Miyajima<sup>3</sup>, Makoto Usami<sup>1</sup>, Yuko Sekino<sup>1</sup>, Taku Matsushita<sup>2</sup> and Seiichi Ishida<sup>1</sup>

<sup>1</sup>Division of Pharmacology, National Institute of Health Sciences, 1-18-1 Kamiyoga, Setagaya-ku, Tokyo 158-8501, Japan

<sup>2</sup>Faculty of Biotechnology and Life Science, Sojo University, 4-22-1 Ikeda, Nishi-ku, Kumamoto 860-0082, Japan

<sup>3</sup>Division of Medical Devices, National Institute of Health Sciences, 1-18-1 Kamiyoga, Setagaya-ku, Tokyo 158-8501, Japan

<sup>4</sup>Present address: Division of Translational Research, Exploratory Oncology Research & Clinical Trial Center, National Cancer Center, 5-1-1 Tsukiji, Chuo-ku, Tokyo 104-0045, Japan

(Received May 19, 2014; Accepted July 6, 2014)

**ABSTRACT** — The liver is the central organ of metabolism, but its function varies during development from fetus to adult. In this study, we comprehensively analyzed and compared metabolites in fetal and adult hepatocytes, the major parenchymal cell in the liver, from human donors. We identified 211 metabolites (116 anions and 95 cations) by capillary electrophoresis-time-of-flight mass spectrometry (CE-TOFMS) in the hepatocytes cultured *in vitro*. Principal component analysis and hierarchical clustering analysis of the relative amounts of metabolites clearly classified hepatocytes into 2 groups that were consistent with their origin, i.e., the fetus and adult. The amounts of most metabolites in the glycolysis/glyconeogenesis pathway, tricarboxylic acid cycle and urea cycle were lower in fetal hepatocytes than in adult hepatocytes. These results suggest different susceptibility of the fetal and adult liver to toxic insults affecting energy metabolism.

**Key words:** Metabolome, CE-TOFMS, Human fetal hepatocytes, Human adult hepatocytes

### INTRODUCTION

The liver is the central organ of human metabolism. The liver performs several complex reactions such as plasma protein synthesis, bile production, nutrient metabolism, energy metabolism, and disposal of waste products of intermediary metabolism. In addition, the liver performs detoxification of xenobiotic compounds through phase I and II biotransformation (Arias *et al.*, 2009).

Hepatocytes are the predominant cell type in the liver, accounting for approximately 70% of the mass of the adult organ. Hepatocytes, along with biliary epithelial cells, are derived from the embryonic endoderm, while stromal cells, stellate cells, Kupffer cells and blood vessels, are of mesodermal origin (Zaret, 2008; Zhao and Duncan, 2005).

The fetal liver is important for development, and its function is distinct from that of the adult liver, functioning primarily as a hematopoietic organ. Chinnici *et al.* (2014) reported that cell suspensions obtained after collagenase digestion of human fetal livers contained approximate-

ly 35% of hepatocytic/epithelial lineage cells, while the remaining cells were mainly erythroid cells. In rodents, fetal hepatocytes are glycolytic and have few mitochondria, suggesting that their energy production is lower than that of adult hepatocytes (Burch *et al.*, 1963; Oliver *et al.*, 1983; Vergonet *et al.*, 1970). A comparison of metabolic function between rat fetal and adult hepatocytes revealed lower activity of key metabolic enzymes in the fetal hepatocytes, including phosphoenolpyruvate carboxykinase and glucose 6-phosphatase for gluconeogenesis, carnitine palmitoyltransferase I and medium-chain acyl-CoA dehydrogenase for fatty acid oxidation, and cytochrome c and  $\beta$ -ATP synthase for mitochondrial energy metabolism (Sharma *et al.*, 2008).

It is also known that the expression of liver-specific genes changes transcriptionally and post-transcriptionally during rat development (Panduro *et al.*, 1987). In humans, several cytochrome P450 enzymes such as CYP1A1, 1A2, 2A6, 2C9, 2E1, and 3A4 were expressed in adult livers, whereas fewer forms of cytochrome P450, namely CYP1A1 and 3A7, were detected in fetal livers

Correspondence: Seiichi Ishida (E-mail: ishida@nihs.go.jp)

(Shimada *et al.*, 1996).

In recent years, comprehensive transcriptome analysis of rat liver and primary cultured hepatocytes treated with several chemicals was carried out and the gene expression database was used for identification of predictive biomarkers for drug-induced toxicity at or before the pre-clinical stage of drug development (Uehara *et al.*, 2010).

The metabolome is the complete set of small molecules (metabolites) in cells in a particular physiological condition and considered to be closely related to the phenotype. Thus, metabolome analysis plays a critical role in understanding complex biochemical and biological systems (Delneri *et al.*, 2001).

Recently, metabolome analysis using capillary electrophoresis-mass spectrometry (CE-MS) has been developed (Monton and Soga, 2007) and applied to the characterization of ionic metabolites from several diseases, including cancer (Hirayama *et al.*, 2009; Kami *et al.*, 2013).

Global metabolome analysis of liver has been performed in several animal models. The differences of metabolic profile in an alcoholic fatty liver in zebrafish were analyzed by proton nuclear magnetic resonance spectroscopy and gas chromatography-mass spectrometry (GC-MS) (Jang *et al.*, 2012). Metabolome profile alterations in fatty liver induced by a high-fat diet in rats were analyzed by GC-MS (Xie *et al.*, 2010). The metabolic profile changes in the liver were also analyzed in aging mice (Houtkooper *et al.*, 2011) and undernourished neonate mice (Preidis *et al.*, 2014). In humans, metabolic profiling and systems biological approaches were used to elucidate the mechanisms of metabolic syndrome and fatty liver disease (Dumas *et al.*, 2014). However, metabolome analysis of prenatal or neonatal human liver has not been investigated.

In this study, to clarify the differences of the basal metabolic functions along with the development of the liver, *in vitro* cultured human fetal and adult hepatocytes were compared by metabolome analysis using capillary electrophoresis time-of-flight mass spectrometry (CE-TOFMS).

## MATERIALS AND METHODS

### Cells and culture conditions

Human fetal hepatocytes (Hc cells, CS-ABI-3716) were purchased from DS Pharma Biomedical (Osaka, Japan). Hc cells were originally prepared from six normal fetal livers (gestation average 16 weeks) by Applied Cell Biology Research Institute (Kirkland, WA, USA). The cells were maintained in CS-C medium kit R (DS Pharma Biomedical) as described previously (Matsushita *et al.*, 2003). The Hc cells were divided into three aliquots that

were cultured separately.

Primary human hepatocytes (HEP220) from three adult donors were purchased from Biopredic International (Rennes, France). The primary human hepatocytes were obtained from patients undergoing resection for primary or secondary tumors, and isolated by collagenase perfusion of histologically normal liver fragment. Patient information is listed in Supplementary Table S1. The cells were maintained in Incubation Medium (MIL214; Biopredic International).

### Metabolite extraction

Ionic metabolites were extracted from  $2\text{--}3 \times 10^6$  cells of human fetal and adult hepatocytes. Cells were washed twice with 5% mannitol solution and suspended in 1 mL of cold methanol containing 10  $\mu\text{M}$  internal standards (Human Metabolome Technologies, Inc., Yamagata, Japan). The number of cells in the same culture condition was counted with a haemocytometer. The cell suspension diluted to 2 mL with methanol was mixed with 2 mL of chloroform and 0.8 mL of Milli-Q water. After centrifugation, the separated methanol-water layer was ultrafiltered using an ultrafiltration tube (Ultrafree-MC, UFC3 LCC; Millipore Corporation, Billerica, MA, USA) with a molecular weight cut-off of 5 kDa to remove proteins. The filtrate was evaporated, dissolved in 50  $\mu\text{L}$  of Milli-Q water, and analyzed using CE-TOFMS.

### Measurement of ionic metabolites using the CE-TOFMS system

CE-TOFMS experiments were performed using an Agilent Capillary Electrophoresis System equipped with an Agilent 6210 Time of Flight mass spectrometer, Agilent 1100 isocratic HPLC pump, Agilent G1603A CE-MS adapter kit, and Agilent G1607A CE-ESI-MS sprayer kit (Agilent Technologies, Waldbronn, Germany).

Cationic metabolites were analyzed using a fused silica capillary i.d.  $50 \mu\text{m} \times 80 \text{cm}$ , with Cation Buffer Solution (Human Metabolome Technologies, Inc.) as the electrolyte. The sample was injected at a pressure of 5.0 kPa for 10 sec. The applied voltage was set at 27 kV. Electrospray ionization-mass spectrometry (ESI-MS) was conducted in the positive ion mode, and the capillary voltage was set at 4,000 V. The spectrometer was scanned from  $m/z$  50 to 1,000.

Anionic metabolites were analyzed using a fused silica capillary i.d.  $50 \mu\text{m} \times 80 \text{cm}$ , with Anion Buffer Solution (Human Metabolome Technologies, Inc.) as the electrolyte. The sample was injected at a pressure of 5.0 kPa for 25 sec. The applied voltage was set at 30 kV. ESI-MS was conducted in the negative ion mode, and the cap-

## Metabolome analysis of human fetal and adult hepatocytes

illary voltage was set at 3,500 V. The spectrometer was scanned from  $m/z$  50 to 1,000. Other conditions for CE-TOFMS experiments were described previously (Soga *et al.*, 2007).

**Data analysis**

The raw data obtained by CE-TOFMS were processed with MasterHands software (Human Metabolome Technologies, Inc.; Sugimoto *et al.*, 2010). Peak information including  $m/z$ , migration time (MT) and area was obtained. The migration time of each sample was normalized relative to the internal standards. The resulting relative area values were further normalized based on the total number of cells. Each peak was aligned according to similar migration time on CE and the  $m/z$  value was determined by TOFMS. Metabolites in the samples were identified by comparing the migration time and  $m/z$  ratio with those of authentic standards, in which differences of  $\pm 0.5$  min and  $\pm 10$  ppm were permitted, respectively. Quantitative values of metabolites are the mean  $\pm$  S.D. for 3 replicates.

The relative quantitation data of identified metabolites were imported into GeneSpring GX software (Version 12.0; Agilent Technologies, Santa Clara, CA, USA), and subjected to principal component analysis (PCA). The relative amounts of metabolites were compared by Welch's *t*-test between fetal and adult hepatocytes, with  $p < 0.05$  considered to be statistically significant. Hierarchical clustering analysis and heatmap representations were also performed with GeneSpring GX software.

**RNA isolation and quantitative RT-PCR analysis**

Total RNA was isolated from hepatocytes with TRIzol reagent (Invitrogen, Breda, the Netherlands), followed by purification using the RNeasy Mini Kit (QIAGEN, Hilden, Germany). The concentration and purity of RNA were measured by Nanodrop ND-1000 spectrophotometer (Nyxor Biotech, Paris, France). First-strand cDNA was prepared from 1  $\mu$ g of total RNA using the High-Capacity RNA-to-cDNA Kit (Applied Biosystems, Foster City, CA, USA) with random primers. Real-time PCR assays were performed with the ABI7900 Real Time PCR System (Applied Biosystems) using the TaqMan Gene Expression Assay for ASS1 (argininosuccinate synthase 1, Hs01597989\_g1), ASL (argininosuccinate lyase, Hs00902699\_m1), ARG1 (arginase, Hs00968979\_m1) and OTC (ornithine transcarbamylase, Hs00166892\_m1), according to the manufacturer's instructions. The relative mRNA levels were determined using calibration curves obtained from serial dilutions of the pooled

hepatocyte cDNA. Transcripts of  $\beta$ -actin were quantified as internal controls using TaqMan  $\beta$ -Actin Control Reagent (Applied Biosystems). The *t*-test was applied to the comparison of the average values of mRNA levels of urea cycle enzymes between fetal and adult hepatocytes.

**RESULTS AND DISCUSSION****Metabolome analysis**

We performed metabolome analysis of human fetal and adult hepatocytes using CE-TOFMS. Based on  $m/z$  values and migration times, 211 metabolites (116 anion and 95 cation) were identified (Supplementary Table S2), and visualized on a large-scale metabolome pathway map (Supplementary Fig. S1), using VANTED software (Junker *et al.*, 2006). Using the whole data set of identified metabolites, we performed a principal component analysis (PCA, Fig. 1) and a hierarchical clustering analysis (HCA, Supplementary Fig. S2) to reveal the similarities/dissimilarities of 2 groups regarding variations in metabolite amounts. From the PCA score plot, fetal and adult hepatocytes were separated in the first principal component (PC1, 47% proportion). The PCA plot indicated that the metabolomic profile of the adult hepatocytes was much more heterogeneous than that of the fetal hepatocytes (Fig. 1). This may reflect the individual differences of donor patients. Metabolites with high absolute values of factor loadings for PC1 included amino acids, glycolysis/glyconeogenesis and tricarboxylic acid (TCA) cycle intermediates, and urea cycle intermediates (data not shown). A heat map representation of HCA was per-

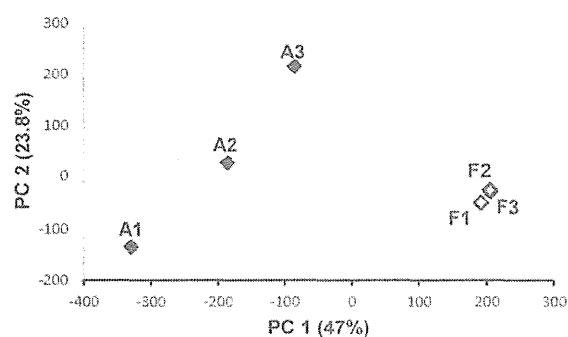


**Fig. 1.** PCA score plot using the normalized metabolomic data from human fetal and adult hepatocytes. The samples were fetal (F1 to F3, open diamonds) and adult (A1 to A3, filled diamonds) hepatocytes. Percentage values indicated on the axes represent the contribution rate of the first (PC1) and the second (PC2) principal components.

**Table 1.** Highly increased or decreased metabolites in the adult hepatocytes compared to those in the fetal hepatocytes

Compound name	Relative area <sup>a</sup>				Fold change (Adult/Fetal)	
	Fetal hepatocytes		Adult hepatocytes		Ratio	<i>P</i> value <sup>b</sup>
	Mean	S.D.	Mean	S.D.		
<i>increased</i>						
Cys	4.3E-04	1.6E-04	2.9E-02	1.1E-02	66.3	0.050
Ornithine	4.2E-03	1.1E-03	2.5E-01	1.1E-01	59.8	0.057
Cysteine glutathione disulphide	6.3E-04	1.3E-04	2.9E-02	2.1E-02	46.1	0.139
Thiaproline	1.9E-03	1.7E-04	6.6E-02	2.6E-02	34.6	0.050
Glycerophosphocholine	5.6E-02	9.8E-03	1.1E+00	1.0E+00	20.6	0.203
<i>O</i> -Phosphoserine	2.1E-04	4.3E-05	4.1E-03	1.3E-03	19.1	0.038
Glycerol 3-phosphate	4.3E-03	3.4E-04	7.5E-02	4.2E-02	17.7	0.098
Urea	1.8E-02	2.3E-03	2.0E-01	1.1E-01	11.1	0.111
Ala	2.4E-01	6.1E-03	2.3E+00	1.2E+00	9.4	0.102
Glucuronic acid	2.9E-04	2.1E-05	2.6E-03	1.7E-03	9.1	0.138
2-Hydroxybutyric acid	3.7E-04	1.1E-04	3.1E-03	2.4E-03	8.4	0.184
3-Hydroxybutyric acid	2.5E-03	3.3E-04	2.1E-02	1.6E-02	8.3	0.189
Guanidoacetic acid	1.5E-03	1.6E-04	1.2E-02	5.1E-03	8.1	0.069
<i>N</i> -Acetylneuraminic acid	1.4E-03	1.1E-04	1.1E-02	9.8E-03	8.0	0.235
Thiamine	1.0E-03	1.7E-04	8.2E-03	3.7E-03	7.8	0.078
Uric acid	1.3E-04	1.9E-05	9.2E-04	7.3E-04	7.2	0.201
Pyridoxamine 5'-phosphate	5.1E-04	5.7E-05	3.7E-03	1.8E-03	7.1	0.094
<i>N</i> <sup>6</sup> -Acetylspermidine	2.5E-03	9.5E-04	1.8E-02	6.4E-03	7.1	0.051
Citrulline	4.3E-03	3.7E-04	2.6E-02	1.0E-02	6.1	0.062
Fumaric acid	5.5E-03	3.7E-04	3.2E-02	2.1E-02	5.8	0.166
Glucaric acid	2.3E-04	5.0E-05	1.2E-03	8.9E-04	5.2	0.200
NADP <sup>+</sup>	2.2E-03	9.7E-05	1.2E-02	8.0E-03	5.2	0.181
<i>decreased</i>						
2-Amino-2-(hydroxymethyl)-1,3-propanediol	3.3E-03	2.5E-04	1.1E-03	3.8E-04	0.3	0.036
2-Oxoisovaleric acid	2.5E-03	2.3E-05	7.6E-04	6.0E-04	0.3	0.040
Gly-Gly	2.2E-03	2.4E-04	6.3E-04	N.A.	0.3	N.A.
Pyridoxine	2.1E-03	1.9E-04	5.9E-04	4.2E-04	0.3	0.091
Carnitine	7.7E-02	1.6E-03	2.1E-02	1.3E-02	0.3	0.015
Gly-Asp	4.5E-03	3.3E-04	1.2E-03	6.9E-04	0.3	0.006
Diethanolamine	5.1E-03	1.6E-03	1.2E-03	1.8E-04	0.2	0.053
Pantothenic acid	3.2E-02	2.3E-03	7.1E-03	6.8E-03	0.2	0.017
Cyclohexylamine	7.2E-03	1.7E-03	1.5E-03	3.4E-04	0.2	0.026
GABA	1.2E-02	9.4E-04	2.7E-03	1.8E-03	0.2	0.004
Phosphocreatine	3.0E-02	4.9E-04	5.5E-03	5.0E-03	0.2	0.014
<i>O</i> -Acetylcarnitine	3.3E-02	1.0E-03	6.0E-03	6.1E-03	0.2	0.015
Fructose 1,6-diphosphate	1.5E-02	1.5E-03	2.4E-03	1.6E-03	0.2	0.009
PRPP	4.4E-03	1.5E-03	6.8E-04	N.A.	0.2	N.A.
$\beta$ -Ala	1.7E-01	1.2E-02	1.0E-02	1.1E-02	0.1	6.0E-05

<sup>a</sup>S.D., standard deviation; N.D., not detected; N.A., not available.

<sup>b</sup>*p* values are calculated by Welch's *t*-test between fetal and adult hepatocytes.

formed on both the metabolite and sample axes. The dendrogram of HCA showed that the adult hepatocytes were well-distinguished from the fetal hepatocytes (Supplementary Fig. S2).

Next, the relative amounts of metabolites were compared between fetal and adult hepatocytes and those that displayed greater than 5-fold or less than 0.3-fold

change in adult hepatocytes were listed (Table 1). Highly increased metabolites in the adult hepatocytes included glycolysis/glyconeogenesis intermediates, some amino acids, and TCA and urea cycle intermediates; decreased metabolites were glycolysis/glyconeogenesis intermediates and metabolites involved in  $\beta$ -oxidation of fatty acids. This trend was consistent with the PCA results described

## Metabolome analysis of human fetal and adult hepatocytes

above. Statistically significant differences in the relative amounts of metabolites between fetal and adult hepatocytes were not found in metabolites that were increased in the adult hepatocytes, because of the variation between adult hepatocyte samples.

## Energy metabolism

We first compared the relative amounts of glycolysis/glyconeogenesis and TCA cycle metabolites between human fetal and adult hepatocytes (Fig. 2), because it was previously reported that fetal hepatocytes are glycolytic and have few mitochondria, suggesting their energy production is lower than that of adult hepatocytes in rat (Burch *et al.*, 1963; Oliver *et al.*, 1983; Vergonet *et al.*, 1970). Our results showed that the levels of glucose 6-phosphate (3.5-fold), fructose 6-phosphate (2.3-fold) and phosphoenolpyruvic acid (2.1-fold) in glycolysis/glyconeogenesis, and fumaric acid (5.8-fold), malic acid (4.8-fold) and succinic acid (3.5-fold) in the TCA cycle were higher in the adult compared with the fetal hepatocytes. In contrast, fructose 1,6-diphosphate in glycolysis/glyconeogenesis was significantly lower (0.2-fold,  $p = 0.009$ ) (Fig. 2, Table 1 and Supplementary Table S2). In addition, among the metabolites involved in  $\beta$ -oxidation of fatty acids, the level of glycerol 3-phosphate which is required for synthesis of diacylglycerol and triacylglycerol, was 17.7-fold higher in the adult compared with the fetal hepatocytes, whereas levels of carnitine and *O*-acetylcarnitine which are required for transport of fatty acids into mitochondria from the cytoplasm, were lower (0.3-fold,  $p = 0.015$  for carnitine, and 0.2-fold,  $p = 0.015$  for *O*-acetylcarnitine, respectively) (Table 1). These results are consistent with previous findings that fetal hepatocytes are glycolytic and possess low mitochondrial activity, and suggest that the pathways of glyconeogenesis and  $\beta$ -oxidation of fatty acid are activated in adult hepatocytes. In fact, the fetus depends on the umbilical supply of glucose via the placenta. Under physiological condition, glucose is not only oxidized to  $\text{CO}_2$ , but also used to synthesis of new structural components and energy storage materials such as glycogen and fat (Fowden, 1994).

## Urea cycle

The relative amounts of urea cycle metabolites were compared between fetal and adult hepatocytes (Fig. 3). The relative amounts of ornithine (59.8-fold), urea (11.1-fold) and citrulline (6.1-fold) were higher in adult compared to fetal hepatocytes (Table 1). The expression levels of urea cycle enzymes were measured by real-time PCR assays and compared between fetal and adult

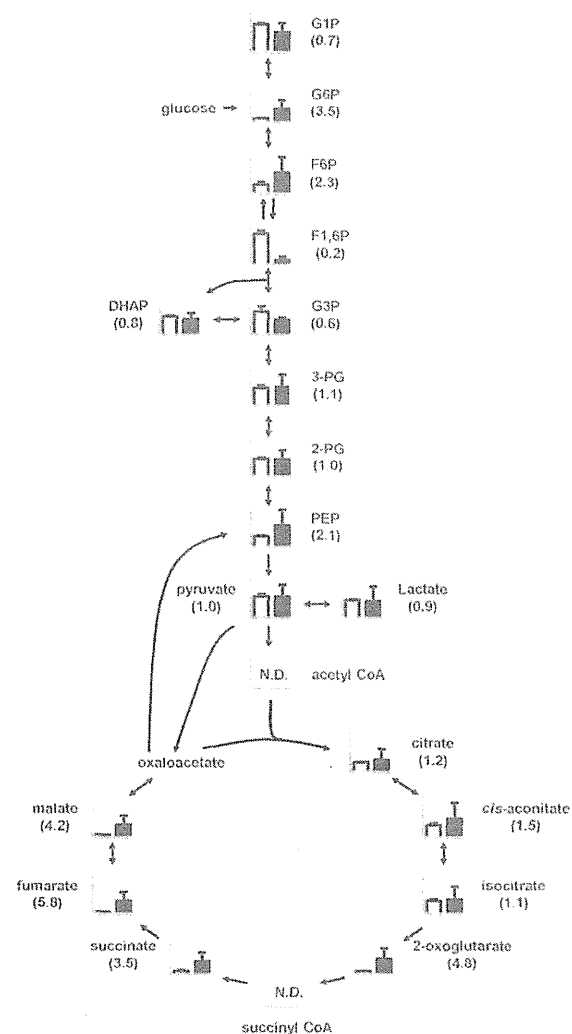


**Fig. 2.** Comparison of relative amounts of glycolysis and TCA cycle-related metabolites in human fetal (open box) and adult (closed box) hepatocytes using CE-TOFMS. N.D. indicates "not detected". The columns represent relative average amounts and error bars indicate SD. Numbers below the metabolite name represent the ratio of relative amounts of metabolites from the adult hepatocytes to those from the fetal hepatocytes. The abbreviations are as follows: G1P, glucose 1-phosphate; G6P, glucose 6-phosphate; F6P, fructose 6-phosphate; F1,6P, fructose 1,6-diphosphate; DHAP, dihydroxyacetone phosphate; G3P, glyceraldehyde 3-phosphate; 3-PG, 3-phosphoglycerate; 2-PG, 2-phosphoglycerate; PEP, phosphoenolpyruvate.

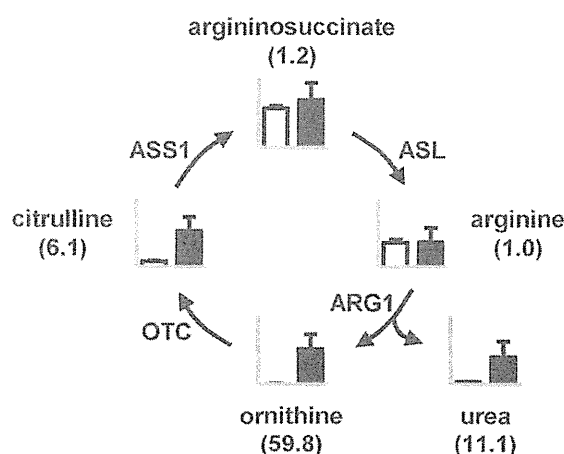


**Fig. 3.** Comparison of relative amounts of urea cycle metabolites in human fetal (open box) and adult (closed box) hepatocytes using CE-TOFMS. The columns represent relative average amounts and error bars indicate SD. Numbers below the metabolite name represent the ratio of relative amounts of metabolites from the adult hepatocytes to those from the fetal hepatocytes. The abbreviations are as follows: ASS1, argininosuccinate synthase 1; ASL, argininosuccinate lyase; ARG1, arginase; OTC, ornithine transcarbamylase.

hepatocytes (Fig. 4). The results showed that the expression levels of ASS1 and ASL were significantly higher in the adult compared to the fetal hepatocytes (2.6-fold,  $p = 0.014$  for ASS1, and 10.4-fold,  $p = 0.027$  for ASL, respectively). Moreover, expression of ARG1 and OTC was detected only in the adult, and not in the fetal hepatocytes. These results indicated that the adult hepatocytes could metabolize the ammonium produced during amino acid metabolism through the urea cycle, whereas the fetal hepatocytes could not.

The lower levels of the urea cycle and TCA cycle metabolites in the fetal hepatocytes are closely related to mitochondrial function. The numbers of mitochondria in mouse hepatocytes were low in the prenatal stage and increased through development and aging of animals (Nagata, 2006). This indicates that energy metabolism differs in fetal and adult hepatocytes and is consistent with previous findings that fetal hepatocytes are glycolytic (Vergonet *et al.*, 1970).

The liver is the first site of contact with xenobiotics, it possesses a high metabolic capacity and has been frequently investigated as a target of toxicity. In adults, the mechanisms of hepatotoxicity are well understood for

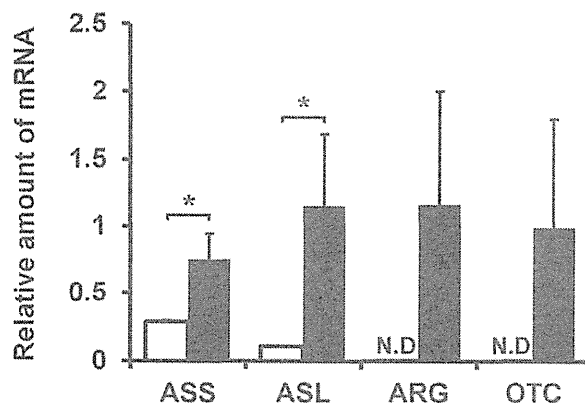


**Fig. 4.** Quantification of mRNA of urea cycle enzymes by TaqMan real-time RT-PCR in human fetal (open box) and adult (closed box) hepatocytes. mRNA expression levels of urea cycle enzymes were normalized with  $\beta$ -actin mRNA levels. The results indicate the mean  $\pm$  S.D. \*,  $p < 0.05$  and N.D., not detected. The abbreviations are as in Fig. 3.

many hepatotoxicants. However, it is known that the sensitivity of fetal hepatocytes to chemical compounds is distinct from that of adult hepatocytes (Shankar and Mehendale, 2010). Most drugs and xenobiotics have molecular weight less than 500 Da and easily cross the placenta to enter the fetal compartment (Evans and Ganjam, 2011). Although systems for evaluating the toxicity of several drug and chemical compounds have been studied for adult liver, such systems have not been elucidated for prenatal or neonatal human liver. Progressive changes in the production of liver-specific enzymes and proteins during normal development generally occur at three specific developmental stages: (1) late gestation, (2) at or directly following birth, and (3) just prior to weaning (Greengard, 1977). We are now proceeding with experiments to construct evaluation systems for toxicity of drugs and chemical compounds in the prenatal period, based on the differences of basal metabolic functions between fetal and adult hepatocytes.

In conclusion, comprehensive metabolome analysis of human fetal and adult hepatocytes was performed by CE-TOFMS and 211 ionic metabolites (116 anion and 95 cation) were identified. Comparison of the relative amounts of metabolites between fetal and adult hepatocytes showed that some metabolites in glycolysis/glyconeogenesis, the TCA cycle and the urea cycle were lower in fetal hepatocytes than in adult hepatocytes. These results provide useful, fundamental information for stud-



ies on the basal metabolic functions of human fetal and adult hepatocytes.

#### ACKNOWLEDGMENT

This work was supported by a Health and Labor Science Research Grant from the Ministry of Health, Labor and Welfare in Japan.

**Conflict of interest**—The authors declare that there is no conflict of interest.

#### REFERENCES

- Arias, I., Wolkoff, A., Boyer, J., Shafritz, D., Fausto, N., Alter, H. and Cohen, D. (2009): *The Liver: Biology and Pathobiology*, 5th edition. Wiley-Blackwell, New Jersey.
- Burch, H.B., Lowry, O.H., Kuhlman, A.M., Skerjance, J., Diamant, E.J., Lowry, S.R. and Von Dippe, P. (1963): Changes in patterns of enzymes of carbohydrate metabolism in the developing rat liver. *J. Biol. Chem.*, **238**, 2267-2273.
- Chinnici, C.M., Timoneri, F., Amico, G., Pietrosi, G., Vizzini, G., Spada, M., Pagano, D., Gridelli, B. and Conaldi, P.G. (2014): Characterization of liver-specific functions of human fetal hepatocytes in culture. *Cell Transplant.*, DOI:10.3727/096368914X680082.
- Delneri, D., Brancia, F.L. and Oliver, S.G. (2001): Towards a truly integrative biology through the functional genomics of yeast. *Curr. Opin. Biotechnol.*, **12**, 87-91.
- Dumas, M.E., Kinross, J. and Nicholson, J.K. (2014): Metabolic phenotyping and systems biology approaches to understanding metabolic syndrome and fatty liver disease. *Gastroenterology*, **146**, 46-62.
- Evans, T.J. and Ganjam, V.K. (2011): Reproductive anatomy and physiology. In *Reproductive and Developmental Toxicology*. (Gupta R.C., ed.), pp.7-32. Academic Press/ Elsevier, Inc., New York.
- Fowden, A.L. (1994): Fetal metabolism and energy balance. In *Textbook of Fetal Physiology*. (Thorburn, G.D. and Harding, R., ed.), pp.70-82, Oxford Medical Publications, Oxford.
- Greengard, O. (1977): Enzymic differentiation of human liver: comparison with the rat model. *Pediatr. Res.*, **11**, 669-676.
- Hirayama, A., Kami, K., Sugimoto, M., Sugawara, M., Toki, N., Onozuka, H., Kinoshita, T., Saito, N., Ochiai, A., Tomita, M., Esumi, H. and Soga, T. (2009): Quantitative metabolome profiling of colon and stomach cancer microenvironment by capillary electrophoresis time-of-flight mass spectrometry. *Cancer Res.*, **69**, 4918-4925.
- Houtkooper, R.H., Argmann, C., Houten, S.M., Cantó, C., Jenjina, E.H., Andreux, P.A., Thomas, C., Doenlen, R., Schoonjans, K. and Auwerx, J. (2011): The metabolic footprint of aging in mice. *Sci. Rep.*, **134.10.1038/srep00134**.
- Jang, Z.H., Chung, H.C., Ahn, Y.G., Kwon, Y.K., Kim, J.S., Ryu, J.H., Ryu, D.H., Kim, C.H. and Hwang, G.S. (2012): Metabolic profiling of an alcoholic fatty liver in zebrafish (*Danio rerio*). *Mol. Biosyst.*, **8**, 2001-2009.
- Junker, B.H., Klukas, C. and Schreiber, F. (2006): VANTED: A system for advanced data analysis and visualization in the context of biological networks. *BMC Bioinformatics*, **7**, 109.
- Kami, K., Fujimori, T., Sato, H., Sato, M., Yamamoto, H., Ohashi, Y., Sugiyama, N., Ishihama, Y., Onozuka, H., Ochiai, A., Esumi, H., Soga, T. and Tomita, M. (2013): Metabolomic profiling of lung and prostate tumor tissues by capillary electrophoresis time-of-flight mass spectrometry. *Metabolomics*, **9**, 444-453.
- Matsushita, T., Nakano, K., Nishikura, Y., Higuchi, K., Kiyota, A. and Ueoka, R. (2003): Spheroid formation and functional restoration of human fetal hepatocytes on poly-L-amino acid-coated dishes after serial proliferation. *Cytotechnology*, **42**, 57-66.
- Monton, M.R. and Soga, T. (2007): Metabolome analysis by capillary electrophoresis-mass spectrometry. *J. Chromatogr. A*, **1168**, 237-246.
- Nagata, T. (2006): Electron microscopic radioautographic study on protein synthesis in hepatocyte mitochondria of aging mice. *ScientificWorldJournal*, **6**, 1583-1598.
- Oliver, I.T., Martin, R.L., Fisher, C.J. and Yeoh, G.C. (1983): Enzymic differentiation in cultured foetal hepatocytes of the rat. Induction of serine dehydratase activity by dexamethasone and dibutyryl cyclic AMP. *Differentiation*, **24**, 234-238.
- Panduro, A., Shalaby, F. and Shafritz, D.A. (1987): Changing patterns of transcriptional and post-transcriptional control of liver-specific gene expression during rat development. *Genes Dev.*, **1**, 1172-1182.
- Preidis, G.A., Keaton, M.A., Campeau, P.M., Bessard, B.C., Conner, M.E. and Hotez, P.J. (2014): The undernourished neonatal mouse metabolome reveals evidence of liver and biliary dysfunction, inflammation, and oxidative stress. *J. Nutr.*, **144**, 273-281.
- Shankar, K. and Mehendale, H.M. (2010): Developmental toxicology of the liver. In *Reproductive Toxicology*, third edition. (Kapp, Jr., R.W. and Tyl, R.W., ed.), pp.205-222, Informa Healthcare, London.
- Sharma, N., Schloss, R. and Yarmush, M. (2008): What came first: fully functional or metabolically mature liver? *Crit. Rev. Biomed. Eng.*, **36**, 413-439.
- Shimada, T., Yamazaki, H., Mimura, M., Wakamiya, N., Ueng, Y.F., Guengerich, F.P. and Inui, Y. (1996): Characterization of microsomal cytochrome P450 enzymes involved in the oxidation of xenobiotic chemicals in human fetal liver and adult lungs. *Drug Metab. Dispos.*, **24**, 515-522.
- Soga, T., Ishikawa, T., Igarashi, S., Sugawara, K., Kakazu, Y. and Tomita, M. (2007): Analysis of nucleotides by pressure-assisted capillary electrophoresis-mass spectrometry using silanol mask technique. *J. Chromatogr. A*, **1159**, 125-133.
- Sugimoto, M., Wong, D.T., Hirayama, A., Soga, T. and Tomita, M. (2010): Capillary electrophoresis mass spectrometry-based saliva metabolomics identified oral, breast and pancreatic cancer-specific profiles. *Metabolomics*, **6**, 78-95.
- Uehara, T., Ono, A., Maruyama, T., Kato, I., Yamada, H., Ohno, Y. and Urushidani, T. (2010): The Japanese toxicogenomics project: application of toxicogenomics. *Mol. Nutr. Food Res.*, **54**, 218-227.
- Vergonet, G., Hommes, F.A. and Molenaar, I. (1970): A morphometric and biochemical study of fetal and adult rat liver cells, with special reference to energy metabolism. *Biol. Neonate*, **16**, 297-305.
- Xie, Z., Li, H., Wang, K., Lin, J., Wang, Q., Zhao, G., Jia, W. and Zhang, Q. (2010): Analysis of transcriptome and metabolome profiles alterations in fatty liver induced by high-fat diet in rat. *Metabolism*, **59**, 554-560.
- Zaret, K.S. (2008). Genetic programming of liver and pancreas progenitors: lessons for stem-cell differentiation. *Nat. Rev. Genet.*, **9**, 329-340.
- Zhao, R. and Duncan, S.A. (2005). Embryonic development of the liver. *Hepatology*, **41**, 956-967.



**SHORT COMMUNICATION**

# Simple *in vitro* migration assay for neural crest cells and the opposite effects of all-*trans*-retinoic acid on cephalic- and trunk-derived cells

Makoto Usami<sup>1</sup>, Katsuyoshi Mitsunaga<sup>2</sup>, Tomohiko Irie<sup>1</sup>, Atsuko Miyajima<sup>3</sup>, and Osamu Doi<sup>4</sup>

Divisions of <sup>1</sup>Pharmacology and <sup>3</sup>Medical Devices, National Institute of Health Sciences, Tokyo, <sup>2</sup>School of Pharmaceutical Sciences, Toho University, Chiba, and <sup>4</sup>Laboratory of Animal Reproduction, United Graduate School of Agricultural Science, Gifu University, Gifu, Japan

**ABSTRACT** Here, we describe a simple *in vitro* neural crest cell (NCC) migration assay and the effects of all-*trans*-retinoic acid (RA) on NCCs. Neural tubes excised from the rhombencephalic or trunk region of day 10.5 rat embryos were cultured for 48 h to allow emigration and migration of NCCs. Migration of NCCs was measured as the change in the radius (radius ratio) calculated from the circular spread of NCCs between 24 and 48 h of culture. RA was added to the culture medium after 24 h at embryotoxic concentrations determined by rat whole embryo culture. RA (10 μM) reduced the migration of cephalic NCCs, whereas it enhanced the migration of trunk NCCs, indicating that RA has opposite effects on these two types of NCCs.

**Key Words:** developmental toxicity, embryo, migration assay, neural crest cell, rat

## INTRODUCTION

Invertebrate development, neural crest cells (NCCs) migrate from the neural primordium throughout the embryo and contribute to morphogenesis (Douarin and Kalcheim 1999). Malfunction of NCCs leads to dysmorphologies, tumors, and syndromes called neurocristopathies (Hall 2009). In developmental toxicology, it has been proposed that altered migration of cephalic NCCs induced by chemicals leads to fetal malformation. For example, retinoic acids and fluconazole inhibited the migration of cephalic NCCs, causing branchial abnormalities in cultured rat and mouse embryos (Pratt et al. 1987; Menegola et al. 2004). These abnormalities are considered to result in *in vivo* craniofacial malformations, such as the cleft palate, cleft lip, micrognathia, and thymic agenesis (Hall 2009).

However, the effects of developmental toxicants on the migration of NCCs in mammals have not been fully investigated because no convenient experimental methods are available. Migration of NCCs is usually examined by time-lapse video imaging of *in vitro* cultured cells (Fuller et al. 2002) or *in vivo* fluorescently labeled cells (Kawakami et al. 2011). These methods are time-consuming and are not suitable for developmental toxicity investigations of chemicals.

In the present study, we have described a simple migration assay that enables investigation of the effects of chemicals on rat NCCs. Cephalic or trunk NCCs were cultured as emigrants from isolated neural tubes of day 10.5 rat embryos. The cultured NCCs were

exposed to test chemicals for 24 to 48 h, and their migration was determined as the change in the radius calculated from the circular spread of the NCCs during exposure. By using this assay method, we found that RA has opposite effects on the migration of cephalic and trunk NCCs.

## MATERIALS AND METHODS

### Animals

Wistar rats (Crj:WI; Charles River Japan, Kanagawa, Japan) were used in these assays. Pregnant rats were obtained by mating female and male rats overnight, and the plug day was designated as day 0.5 of gestation. All the animal experiments were performed in accordance with the guidelines for animal experiments of the National Institute of Health Sciences.

### Rat whole embryo culture

Rat embryos on day 10.5 of gestation were cultured for 24 h by the roller bottle method as described previously (Usami et al. 2008). All-*trans*-retinoic acid (RA, CAS 302-79-4; Wako Pure Chemical Industries, Osaka, Japan) was dissolved in dimethyl sulfoxide before adding it to the culture medium, which was rat serum. Control embryos were cultured in the presence of the same concentration of dimethyl sulfoxide.

### NCC culture

Neural crest cells were cultured as emigrated cells from the neural tubes of day 10.5 rat embryos, as outlined in Figure 1A. Neural tubes were excised from the rhombencephalic or trunk region of the embryos in Hanks' balanced salts solution with sharpened tungsten needles. The excised neural tubes (approximately 0.7 mm long) were cut open dorsally and attached to the 35-mm cultured dishes (BD Primaria; Becton Dickinson, Franklin Lakes, NJ, USA) containing 2 mL of Dulbecco's Modified Eagle Medium with high glucose (DMEM; Gibco, Life Technologies, Carlsbad, CA, USA) and 10% (v/v) fetal bovine serum (Gibco) (Fig. 1B, C). The dishes were incubated at 37°C with 5% CO<sub>2</sub> for 48 h. After 24 h of culture, the medium was replaced with medium containing RA dissolved in dimethyl sulfoxide (final concentration, 0.1% v/v).

### Observation and analysis of cultured NCCs

Neural crest cell emigrants from the neural tubes were observed for their attachment to the surface of the culture vessels and the extent of migration. Images of cultured NCCs were recorded digitally with a phase-contrast microscope (BZ-9000; Keyence, Osaka, Japan) after 24 and 48 h of culture. NCCs that did not completely surround the neural tube after 24 h of culture and those cultures in

Correspondence: Makoto Usami, PhD, Division of Pharmacology, National Institute of Health Sciences, 1-18-1, Kamiyoga, Setagaya, Tokyo 158-8501, Japan. Email: usami@nihs.go.jp

Received January 8, 2014; revised and accepted March 31, 2014.

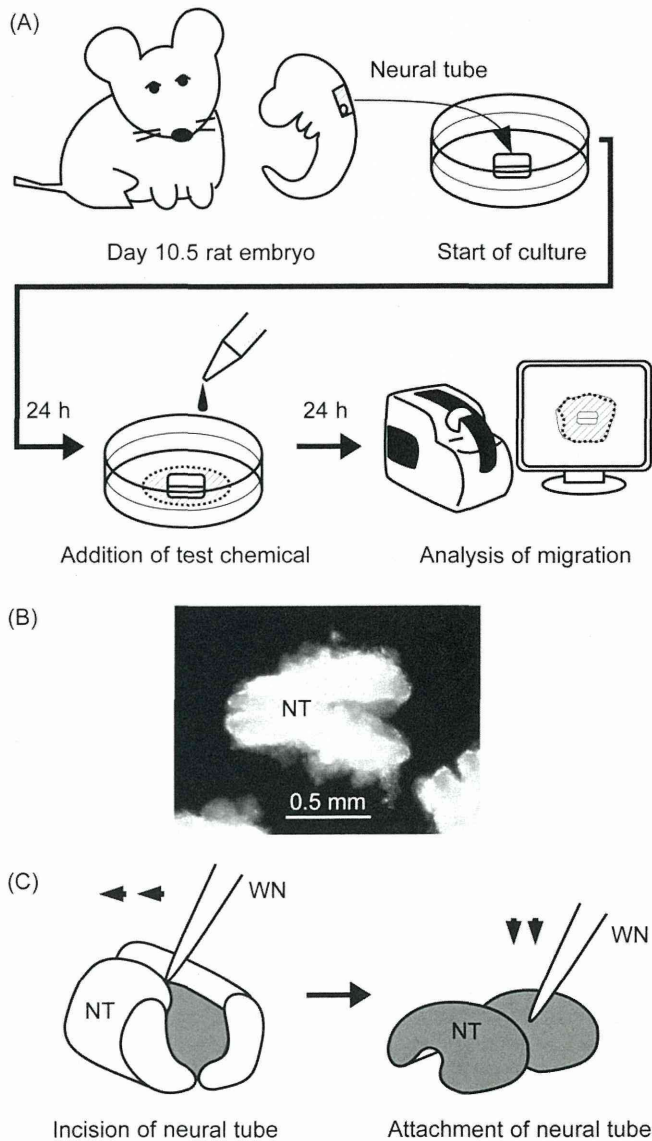


**Fig. 1** Outline of the neural crest cell (NCC) migration assay. (A) Neural tubes were excised from the rhombencephalic region of day 10.5 rat embryos and cultured for 48 h to allow migration of the NCCs. Test chemicals were added to the culture medium after 24 h of culture. Migration indices were calculated as the circular spread of NCCs after 24 and 48 h of culture. (B) Dorsal view of a neural tube prepared for culture. The right side is cranial. (C) Neural tubes were incised dorsally and pressed to the culture plate surface with the outer wall downward using a tungsten needle. It should be noted that the neural tubes became concave outward after the incision. NT, neural tube. WN, tungsten needle.

which the neural tube detached from the surface of the culture vessel before the end of the culture period were omitted from the analyses because they showed little migration.

The migration distance of the NCCs was calculated as the increase in the radius of the circular spread between 24 and 48 h of culture. The digital images of cultured NCCs were analyzed by using ImageJ software (<http://rsb.info.nih.gov/ij/>, 1997–2009; Rasband, W.S., ImageJ, U.S. National Institutes of Health, Bethesda, MD, USA). The outermost NCCs in each of the cultured neural tubes were reconnected with the polygon tool as a rubber

band were placed around the cells, and the pixel count inside the polygon was measured. Considering the polygon as a circle, its radius was calculated as follows:

$$\text{Radius} = \sqrt{\frac{\text{number of pixels in polygon}}{\pi}}.$$

To assess NCC migration, the radius ratio was calculated using the following formula:

$$\text{Radius ratio} = (\text{radius at 48 h} / \text{radius at 24 h}) / 24.$$

This ratio was then normalized to the control to allow for comparisons between experiments.

### Immunocytochemistry

At the end of the culture period, the neural tubes and non-NCCs derived from surrounding tissues were removed with tungsten needles under a stereomicroscope, leaving the emigrated cells in the dish. The emigrated cells were fixed with 4% (w/v) paraformaldehyde in phosphate-buffered saline (PBS) for 20 min, permeated with 0.1% Triton X-100 in PBS for 2 min, and blocked with 3% (w/v) bovine serum albumin (BSA) in PBS for 30 min at room temperature. The treated cells were incubated with primary antibody in 1% (w/v) BSA-PBS for 1 h, and then incubated with a secondary antibody in 1% (w/v) BSA-PBS for 1 h at room temperature. The primary antibodies used were an anti-HNK-1 mouse IgM monoclonal antibody (CBL519; Merck KGaA, Darmstadt, Germany) and an anti-SOX10 mouse IgG monoclonal antibody (MAB2864; R & D Systems, Minneapolis, MN), and the secondary antibodies used were fluorescently labeled anti-mouse (Alexa Fluor 488 goat anti-mouse IgM, A-21042; Invitrogen, Life Technologies) and anti-rabbit (Alexa Fluor 594 goat anti-mouse IgG (H + L), A-11005; Invitrogen) antibodies. To stain the cell nuclei, 4',6-diamidino-2-phenylindole (DAPI, D-1306; Invitrogen) dissolved in methanol (2 mg/mL) was added to the secondary antibody solutions at a concentration of 0.1% (v/v). The immunostained cells were photographed with a fluorescence microscope (BZ-9000, equipped with the DAPI-BP, GFP-BP, and Texas Red filters; Keyence).

### Statistical analysis

Statistical significance of the difference between the experimental groups was examined by the Student's *t*-test or Fisher's exact test.

## RESULTS

### Identification of NCCs

Cells emigrated from explanted rhombencephalic and trunk neural tubes during culture were identified as NCCs by immunocytochemistry of the following marker antigens, HNK-1 (Nagase et al. 2003) on the cell membrane and SOX10 (Kim et al. 2003) in the cell nucleus. The nuclei of the emigrated cells were stained by DAPI and the anti-SOX10 antibody, and the cells were stained by the anti-HNK-1 antibody (Fig. 2A–C). The merged images showed the co-expression of HNK-1 and SOX10 in the emigrated cells at least in the periphery of the circular spread (Fig. 2D). Thus, the emigrated cells were identified as NCCs.

### Analysis of NCC migration

Figure 3A shows images of NCCs after 24 and 48 h of culture. The migration of NCCs was calculated as the difference in the radius of the circular spread of the cells between 24 and 48 h of culture because it was impossible to determine the migration distance from

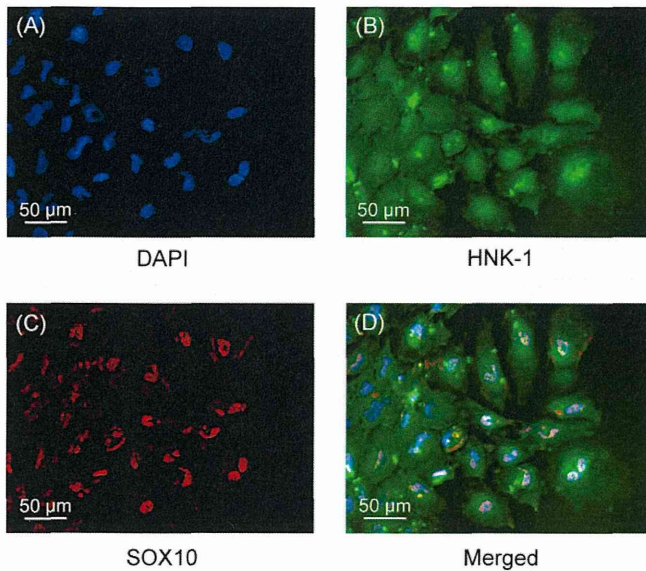


**Fig. 2** Immunocytochemical identification of neural crest cells (NCCs). (A) Nuclear staining with 4',6'-diamidino-2-phenylindole dihydrochloride (DAPI). (B) Staining of the cell membrane with anti-HNK-1 antibody. (C) Staining of nuclei with anti-SOX10 antibody. (D) A merged image of A, B, and C.

the neural tubes since its outline was obscured during culture, and individual NCCs could not be distinguished. The mean migration distance of the NCCs calculated using this method was approximately 500  $\mu\text{m}$  during the 24-h culture period. To evaluate NCC migration, the radius ratio was used because this ratio showed less variability than the radius difference as determined by the coefficient of variation, suggesting the dependence of NCC migration on the size of the explanted neural tubes (Fig. 3B).

#### Effects of RA on cultured rat embryos

Embryotoxic concentrations of RA were determined by rat whole embryo culture to compare RA-induced embryotoxicity to the effects of RA on NCC migration. RA was toxic to cultured rat embryos at concentrations  $\geq 3 \mu\text{M}$ , which caused a reduction in the number of somite pairs and an increased incidence of morphological abnormalities (Table 1). Deformed branchial arches, more specifically, the hypoplastic 3rd branchial arch, were observed at 10  $\mu\text{M}$  RA but not at 3  $\mu\text{M}$  (Fig. 4). These embryotoxic concentrations were comparable to those in the maternal plasma (about 4.5  $\mu\text{g}/\text{mL} = 15 \mu\text{M}$ ) obtained by the administration of a teratogenic dose (10 mg/kg) of RA to mice (Kraft 1992), and the observed abnormalities corresponded to *in vivo* malformations of the ear, eye, and thymus. Based on these results, RA was added at 0, 3, and 10  $\mu\text{M}$  during the 24-h exposure period in the following NCC migration experiments.

#### Effects of RA on NCC migration

Rat NCCs that migrated from the neural tube were exposed to embryotoxic concentrations of RA for 24 h. RA reduced the migration of cephalic NCCs in a concentration-dependent manner, and 10  $\mu\text{M}$  RA reduced the migration by approximately 10% (Fig. 5A). In contrast, RA (10  $\mu\text{M}$ ) enhanced the migration of trunk NCCs by

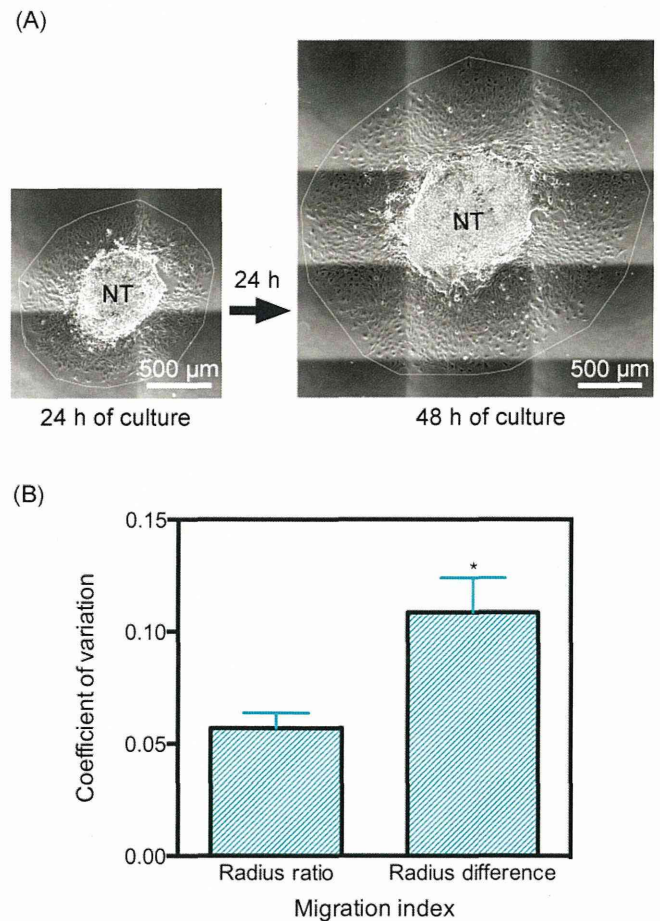


**Fig. 3** Analysis of neural crest cell (NCC) migration. (A) Cultured NCCs were enclosed in a polygon to calculate the migration indices after 24 and 48 h of culture. (B) Comparison of migration indices. The means  $\pm$  standard error of the mean (SEM) of the coefficient of variation from eight control cultures are shown for the migration indices: the radius ratio and the radius difference.

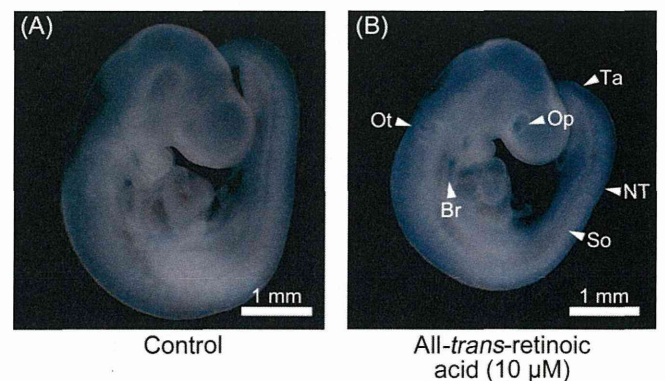


**Fig. 4** Appearance of rat embryos cultured in the presence of all-trans-retinoic acid. Rat embryos after 24 h of culture are shown after removal of the embryonic membranes. Arrowheads indicate deformed organs. Br, branchial arch; NT, neural tube; Op, optic vesicle; Ot, otic vesicle; So, somite; Ta, tail.